

Part III
Extreme Weather

*Chapter 15***Potential Vorticity Structure and Propagation Mechanism
of Indian Monsoon Depressions**

William R. Boos

*Department of Geology and Geophysics, Yale University,
New Haven, CT 06511, USA
billboos@alum.mit.edu*

Brian E. Mapes

*Rosenstiel School of Marine and Atmospheric Sciences, University of Miami,
Miami, FL 33149, USA*

Varun S. Murthy

*Department of Geology and Geophysics, Yale University,
New Haven, CT 06511, USA*

Indian monsoon depressions are synoptic-scale storms that form primarily over the Bay of Bengal and propagate westward over the subcontinent, producing a large fraction of India's total summer precipitation. We recently showed that, contrary to long-standing ideas, the westward propagation of Indian monsoon depressions is accomplished primarily by horizontal adiabatic advection of potential vorticity (PV), not by vortex stretching or diabatic PV generation that occurs in the region of quasi-geostrophic ascent southwest of the vortex center. This chapter extends that work by using several reanalysis products to examine case studies of Indian monsoon depressions. In all reanalyses examined, monsoon depressions have maximum PV in the middle troposphere, at higher altitudes than the level of maximum relative vorticity. The horizontal structure of mid-tropospheric PV suggests that the axial asymmetry of the vortex that produces the nonlinear westward advection may result at least partly from diabatic heating. Thus, although storm motion is produced primarily by horizontal adiabatic advection, diabatic heating can play an indirect role by shaping the PV field that produces this advection.

1. Introduction

Tropical monsoon circulations contain synoptic-scale cyclonic vortices that produce a large fraction of the annual mean rainfall in many monsoon regions (Yoon and Chen 2005; Berry *et al.* 2012; Hurley and Boos 2015). In the Indian region these vortices are commonly classified as monsoon lows, monsoon depressions, deep depressions, and cyclonic storms based on their surface wind speeds and surface pressure

anomalies (Ramage 1971; India Meteorological Department 2011). Monsoon depressions (hereafter simply referred to as depressions) are the subset of these vortices that have surface wind speeds of $8\text{--}13\text{ m s}^{-1}$ and typical central surface pressure anomalies of $4\text{--}10\text{ hPa}$. Each year, an average of 5–7 depressions are observed during June–September in the Indian monsoon region. These typically form over the Bay of Bengal and travel northwest over the Indian subcontinent, lasting for 3–6 days (Mooley and

Shukla 1987; Sikka 1977). Peak precipitation rates in the average depression are about 50 mm day^{-1} (Yoon and Chen 2005, Boos *et al.* 2015).

Although monsoon depressions are cyclonic vortices located in the tropics, they are distinct from tropical cyclones as traditionally defined. Monsoon depressions have a cold core in the lower troposphere and loosely organized convection with no central core or eyewall (e.g. Sikka 1977; Godbole 1977; Yoon and Chen 2005). In contrast, the U.S. National Hurricane Center defines a tropical cyclone as a warm-core vortex with a closed surface wind circulation about a well-defined center (NHC 2015). Furthermore, monsoon depressions frequently pass over land surfaces without loss of intensity, indicating that, unlike tropical cyclones, they do not maintain their intensity by extracting heat from the ocean via surface evaporative fluxes.

The mechanisms of growth and propagation of Indian monsoon depressions have long been associated with the strong vertical wind shear of the monsoon mean state, or equivalently with that state's strong poleward temperature gradient. The amplification of monsoon depressions to mature intensity has been most commonly attributed to some sort of baroclinic instability, or stable non-modal baroclinic growth, heavily modified by the diabatic effects of moist convection (e.g. Krishnamurti *et al.* 1983, Moorthi and Arakawa 1985, Farrell 1985, Krishnamurti *et al.* 2013). The vertical shear of the monsoon mean state has also been invoked to explain the apparent upstream propagation of Indian monsoon depressions against the low-level monsoon westerlies. Quasi-geostrophic lifting downshear (i.e. to the west) of the low-level vorticity maximum produces convectively coupled ascent and vortex stretching that was argued to shift the vortex westward (Rao and Rajamani 1970; Sanders 1984; Chen *et al.* 2005). For tropical cyclones viewed as potential vorticity (PV) maxima, this propagation mechanism has been called "direct generation of a positive PV tendency by asymmetric heating" (Wu and Wang 2001), because

the downshear precipitation provides a diabatic PV source. Observations have shown that peak precipitation and ascent do occur west of the vortex center in monsoon depressions (Godbole 1977), although the peak ascent typically occurs southwest of the vortex center while storm propagation is to the northwest.

Boos *et al.* (2015) examined the PV tendencies involved in the propagation of Indian monsoon depressions and showed that direct generation of PV by diabatic sources is less important than the horizontal adiabatic advection of the depression's central core of PV by azimuthally asymmetric flow. However, Boos *et al.* (2015) largely assumed that the asymmetric flow accomplishing the horizontal advection originated from interaction of the depression with the planetary vorticity gradient — the so-called "beta drift" that is also thought to play a role in tropical cyclone motion (see Chan 2005 for a review). Boos *et al.* (2015) did not consider the possibility that diabatic heating might generate the azimuthally asymmetric flow that then adiabatically advects the depression to the northwest. That indirect role of diabatic heating was discussed by Wu and Wang (2001) in the context of tropical cyclone motion.

This chapter considers these diabatic and adiabatic mechanisms for the axial asymmetry and thus for the propagation mechanism of Indian monsoon depressions, in the context of two case studies. PV structures are compared across multiple reanalysis products, some of which provide estimates of diabatic heating rates. Our analyses extend the results of Boos *et al.* (2015) by showing that diabatic generation of PV may help produce the asymmetries of the PV field that are responsible for the horizontal adiabatic advection of PV in monsoon depressions.

2. Data and Methods

General characteristics of the propagation of Indian monsoon depressions are first established

by examining a large ensemble of storms as represented in the European Centre for Medium-Range Weather Forecasts (ECMWF) Interim Reanalysis (ERA-Interim; Dee *et al.* 2011) for 1979–2012. ERA-Interim uses a spectral T255 atmospheric model constrained by observations, with 60 vertical levels and gridded output available every 6 hours at a horizontal resolution of roughly $0.7 \times 0.7^\circ$. Depressions are identified and tracked in the ERA-Interim dataset using an automated algorithm (Hodges 1995) to identify propagating 850 hPa relative vorticity maxima having surface wind speeds and sea level pressure anomalies consistent with the India Meteorological Department (IMD) definition of a monsoon depression. Full details of this tracking and selection algorithm are provided in Hurley and Boos (2015). Weaker storms (monsoon lows) and stronger storms (deep depressions and cyclonic storms) are filtered out by these selection criteria.

Individual case studies make use of the ECMWF Year of Tropical Convection (EC-YOTC) analysis (Waliser *et al.* 2012), which is available for May 2008–April 2010. This dataset uses a spectral T799 atmospheric model with 97 vertical levels and gridded output available every 6 hours at a horizontal resolution of $0.25 \times 0.25^\circ$. The EC-YOTC dataset provides tendencies associated with model parameterizations and dynamics during 24-hour forecasts initialized at 1200 UTC daily.

For case studies, comparisons have also been made with other reanalysis products: the NCEP-NCAR reanalysis (Kalnay *et al.* 1996), the Climate Forecast System Reanalysis (CFSR, Saha *et al.* 2010), and the MERRA reanalysis (Reinecker *et al.* 2011). Case study data from these sources were obtained from online aggregations and displayed together using the free Integrated Data Viewer (IDV) software. IDV “bundle” files for reproducing these analyses, freely usable from any networked computer, are available on request from the second author (mapes@miami.edu). Operational analyses from

the NCEP Global Forecast System and the coarse 20th Century reanalysis were also examined, but are not presented here for brevity.

3. Results

3.1. General propagation characteristics

The tracking algorithm identified 159 vorticity maxima with track origins in the region $50\text{--}100^\circ\text{E}$, $0\text{--}30^\circ\text{N}$ during June–Sept. 1979–2012 that can be classified as depressions. Consistent with previous studies (e.g. Mooley and Shukla 1987), genesis occurs primarily over the northern Bay of Bengal, and depressions propagate to the west-northwest with tracks terminating over northern India and surrounding regions (Fig. 1). A fair number of genesis points do fall over land, primarily in and around the eastern Indo-Gangetic plain, and some storms also form over the Arabian Sea. The joint distribution of the zonal and meridional components of

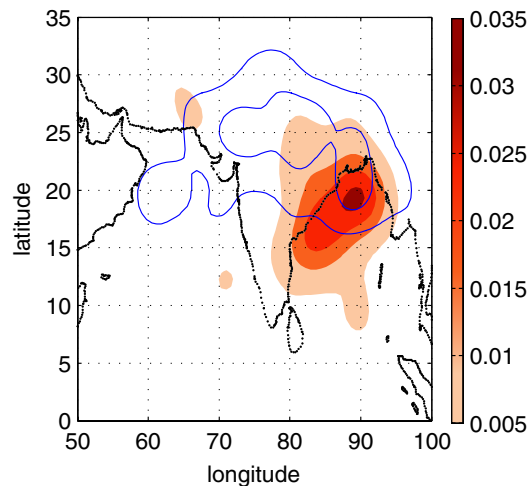


Fig. 1. Shading shows number of depression genesis points per square degree in ERA-Interim per summer season (June–Sept.) after smoothing with a Gaussian kernel having an isotropic standard deviation of 2° . Blue contours show the same quantity but for the endpoints of depression tracks. Contour intervals are 0.01 starting at 0.005 storms per summer per square degree.

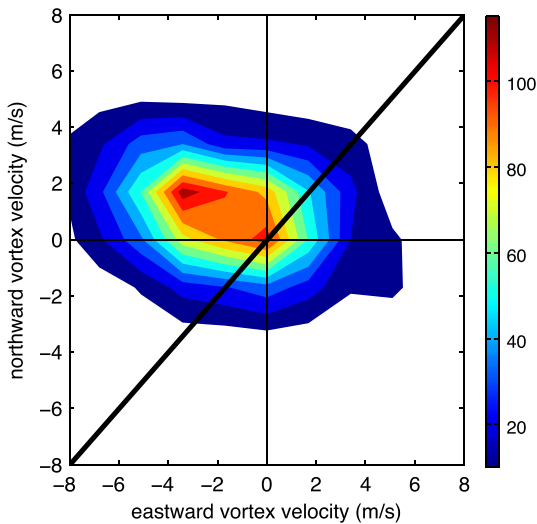


Fig. 2. Joint distribution of depression propagation velocities for all time points in the middle third of every track. Contour interval is a count of 10 starting at 10. Thick black line is the 1:1 line.

the propagation velocity vector, sampled once every 6 hours over the middle third of every depression track, has a mode at a zonal velocity of -3.4 m s^{-1} and a meridional velocity of 1.7 m s^{-1} , which corresponds to propagation to the west-northwest at 3.8 m s^{-1} (Fig. 2). However, the propagation vector varies substantially in magnitude and direction, with some storms even propagating to the southeast, and the mean propagation velocity being -1.5 m s^{-1} and 1.0 m s^{-1} in the zonal and meridional directions, respectively. Both the mode and mean are slower than the westward speed of 5° longitude/day (5.8 m s^{-1}) that is sometimes cited for the propagation speed of Indian monsoon depressions (e.g. Yoon and Huang 2012).

3.2. Vorticity and PV structures

We now examine the vorticity and PV distributions of two individual depressions, one occurring in Sept. 2008 and the other in July 2009. These storms were chosen because they occur during the period of the EC-YOTC dataset, have intensities typical of Indian monsoon

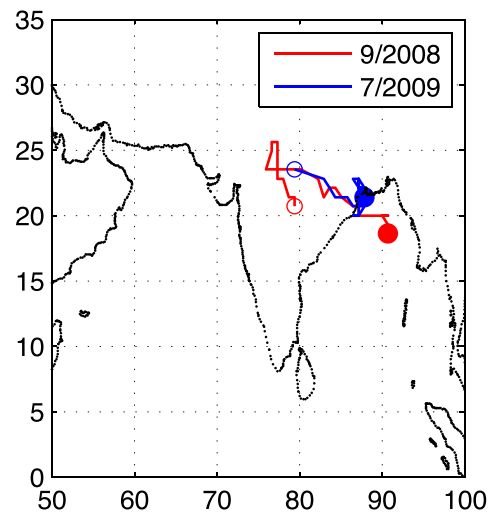


Fig. 3. Tracks of two depressions with genesis points (filled circles) on Sept. 13, 2008 (red) and July 8, 2009 (blue). Track termination points are shown by open circles and occur on Sept. 21, 2008 (red) and July 16, 2009 (blue).

depressions, and propagate in the classic west-northwest direction from their origin points over the northern Bay of Bengal (Fig. 3). When the maximum surface wind speed achieved within 500 km of the storm center is sampled every 6 hours along each track, the 2008 depression is found to have a distribution centered at slightly lower speeds than that associated with all depressions, while the 2009 storm is somewhat stronger (not shown).

The September 2008 case is shown in Fig. 4 near the time it crossed India’s east coast. A second cyclone on the west coast was also present, so the transect was positioned to display them both. Relative vorticity (lower panels) has maximum values in the lower troposphere (the color scale saturates in Fig. 4c), although the vorticity column does extend into the upper troposphere. An enormous increase in detail is seen in the 0.25-degree EC-YOTC product when compared with the 2.5 degree NCEP-NCAR product. Figure 5 shows enlarged transects through the east coast depression of Fig. 4, for relative vorticity (top) and PV (bottom) from

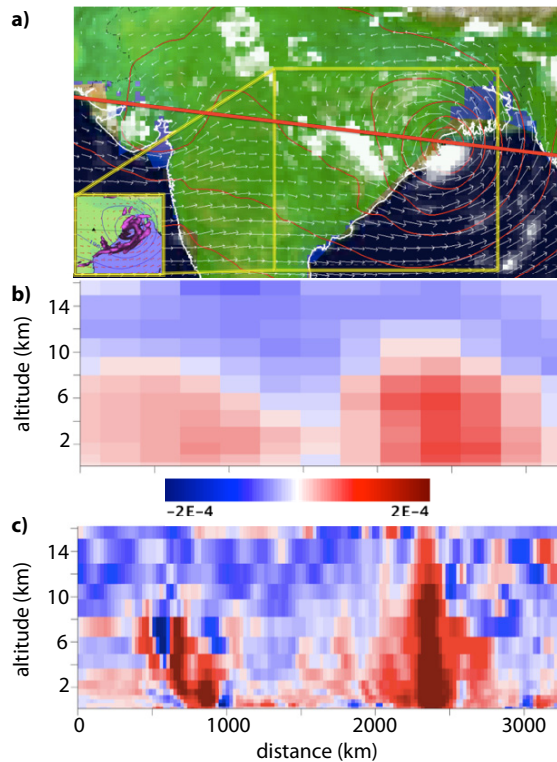


Fig. 4. Depictions of the monsoon cyclone (Bay of Bengal coast) and a secondary cyclone (Arabian Sea coast) on Sept. 16, 2008 at 1200 UTC. (a) Map view with EC-YOTC winds and geopotential contours at 850 hPa, overlain by TRMM 3B42 rainrate product (white shaded pixels). Inset (yellow box) shows a top view of the $PV = 1$ PVU isosurface in the EC-YOTC analysis (magenta). Red line shows the location of the cross sections below. (b) Relative vorticity section in the NCEP-NCAR reanalysis (on a 2.5 degree grid). (c) As in (b) but for the EC-YOTC analysis (on a 0.25 degree grid). Color bar is for both (b) and (c) and has units of s^{-1} .

three different reanalyses. In all three products (EC-YOTC, CFSR, and MERRA), the vertical structure of PV is more top-heavy than that of relative vorticity. This is indicative of the larger static stability in the mid-troposphere, near the melting level, since for monsoon depressions the PV is approximately equal to the product of the vertical component of the absolute vorticity vector and the climatological mean stratification (Boos *et al.* 2015).

The July 2009 case (Fig. 6) is somewhat weaker, but largely confirms the lessons of Figs. 4 and 5. In both cases, precipitation west of the cyclone is seen at the analysis time (1200 UTC; top panels of Figs. 4 and 6). Note that although the July 2009 case had a weaker PV anomaly than the Sept. 2008 case, its peak surface wind speeds were stronger, as represented in ERA-Interim (not shown).

These vorticity and PV structures are typical of those seen in monsoon depressions. To demonstrate this, we show in Fig. 7 the composite mean PV and zonal wind, averaged in a storm-centered coordinate system along the middle third of each of the 159 tracks in ERA-Interim. The maximum PV is clearly centered at 500 hPa, and a weaker secondary maximum is centered around 725 hPa. The PV maximum is located just slightly above the climatological mean zero zonal wind line, although the circulation of the storm is so strong that there is large horizontal shear across the PV maximum. The climatological baroclinicity is evident in the easterly vertical wind shear at the storm center, especially at the highest levels of the troposphere south of the center of the composite depression. Several conclusions can be drawn from these structures: (1) from a PV perspective, one would view depressions as being centered near 500 hPa, well above the lower troposphere where the relative vorticity peaks and the climatological mean flow is eastward; (2) the depression circulation is strong compared to the mean flow (i.e. it is far from the limit of a weak linear anomaly), so that any horizontal advection may be highly nonlinear and it may not be useful to think of depressions being advected by a mean flow. The rest of this chapter is devoted to examination of the mechanism of propagation.

3.3. The central question: is beta drift sufficient?

Boos *et al.* (2015) showed that the mid-tropospheric PV maximum of Indian monsoon

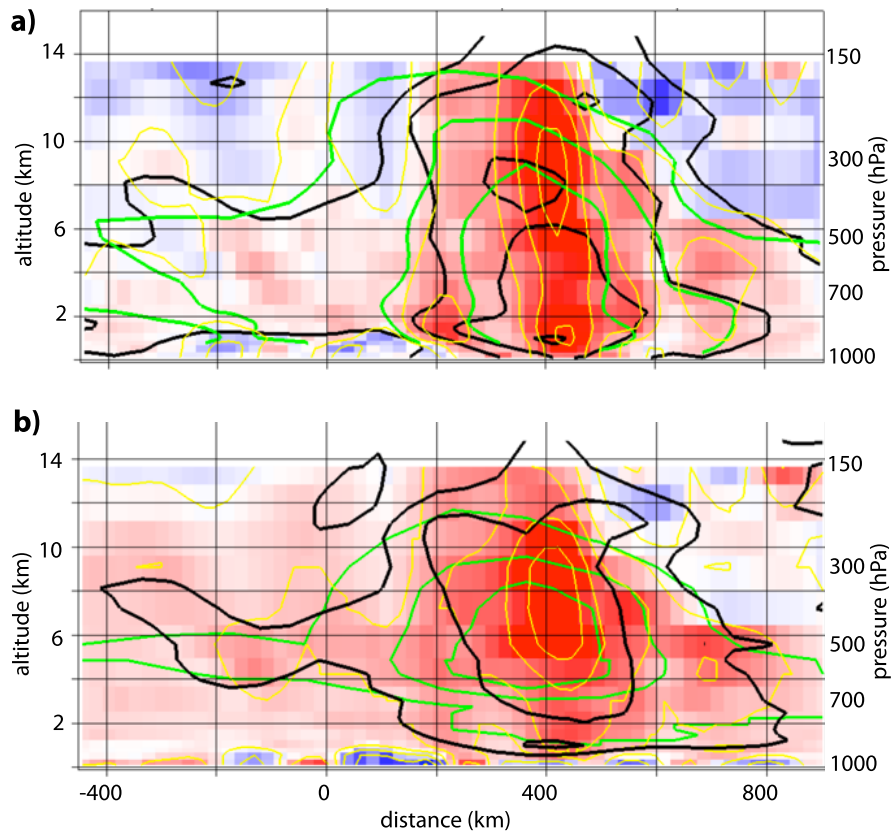


Fig. 5. Cross sections through the Bay of Bengal cyclone shown in Fig. 4, along the same transect. (a) Relative vorticity (contour interval $5 \times 10^{-5} \text{ s}^{-1}$). (b) Potential vorticity (contour interval 0.5 PVU). Color shading (red is positive and blue negative) and yellow contours both show the EC-YOTC analysis, black contours show CFSR, and green contours show MERRA.

depressions moves westward by horizontal adiabatic advection. They demonstrated that, for more than 100 monsoon depressions, the storm motion had a direction and speed consistent with that of the PV-weighted horizontal wind at 500 hPa. Only the total horizontal wind was strong enough to explain the storm motion; the time-mean wind was much too weak at 500 hPa and was in the wrong direction in the lower troposphere. They also used a PV budget for the same Sept. 2008 storm examined here to show that the net Eulerian time tendency of PV was produced primarily by horizontal adiabatic advection, with diabatic PV generation playing only a minor role. Yet how, exactly, does this

horizontal, nonlinear advection produce the net storm motion?

Nonlinear self-advection of vortices on rotating spheres has been well studied in the context of tropical cyclones, where this mechanism of propagation is known as “beta drift” (see reviews by Wang *et al.* 1998, Chan 2005). Beta drift occurs when a cyclonic vortex advects the background vorticity field, which has a poleward gradient, to produce an anomalous cyclone to the west of the original vortex and an anomalous anticyclone to the east. These induced anomalies, called beta gyres, have a circulation that interferes constructively to produce a net wind that advects the center of the

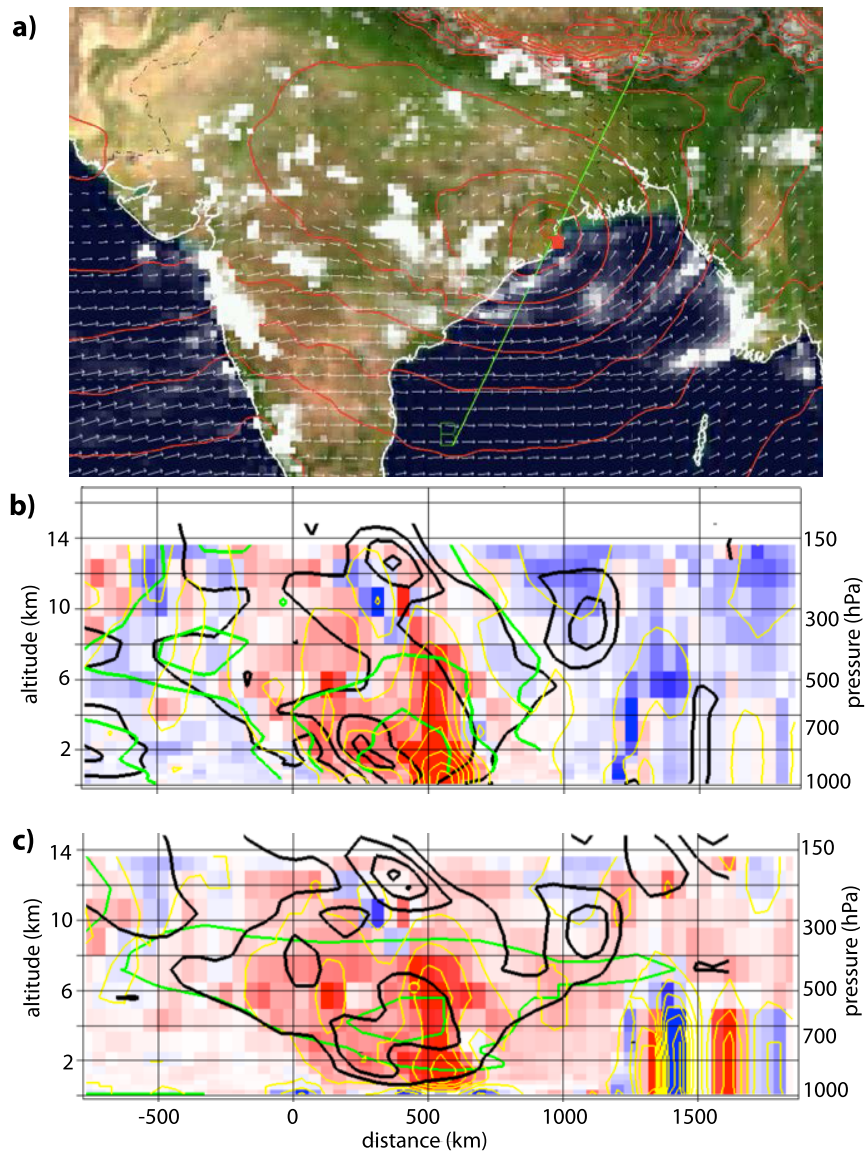


Fig. 6. For the monsoon depression of July 14, 2009 at 1200 UTC, (a) as in Fig. 4a, with the green line marking the transect for which vertical profiles are shown in the next two panels. (b) Relative vorticity, as in Fig. 5b. (c) Potential vorticity, as in Fig. 5c. The lower right region of (b) and (c) lies below the surface of the Himalayas and should be disregarded as it represents non-physical data in the EC-YOTC product.

original vortex. The anomalous gyres are typically rotated by the azimuthally symmetric flow to produce northwestward flow across the original vortex, although there is some sensitivity to the baroclinicity of the vortex, background flow, and other factors.

The existence of asymmetric gyres that advect monsoon depressions to the northwest can be demonstrated through decomposition of the horizontal streamfunction into components that are azimuthally symmetric and asymmetric about the vortex center (e.g. Fiorino and

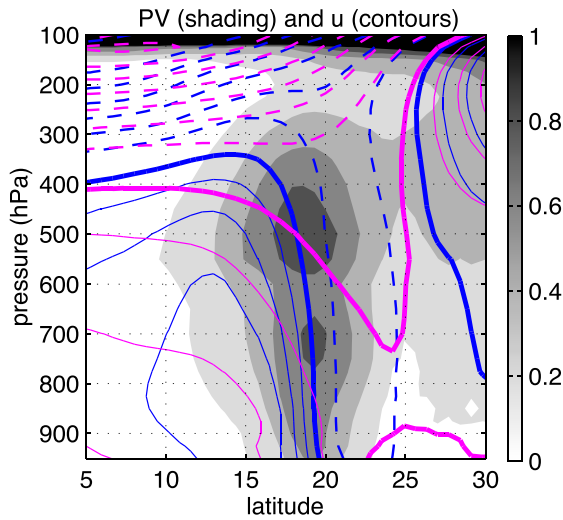


Fig. 7. Storm-centered composite mean PV (gray shading, contour interval of 0.2 PVU), zonal wind (blue contours), and climatological mean zonal wind (magenta contours), all along a single longitude line running through the 850 hPa vortex center. Zonal wind contour interval is 4 m/s with negative values dashed and the zero contour in bold. The climatological mean wind was obtained by sampling a daily climatology (for 1979–2012) along each point of the depression’s track, then averaging in a storm-centered coordinate system to form a composite mean.

Elsberry 1989). For the composite-mean monsoon depression, the part of the 500 hPa streamfunction that is azimuthally asymmetric about the PV maximum (obtained by subtracting the azimuthally symmetric component) shows an anomalous cyclone southwest of the PV maximum and an anomalous anticyclone to the northeast (Fig. 8). These gyres together produce flow toward the northwest over the PV maximum, and have a structure qualitatively consistent with that seen in idealized models of barotropic beta drift (e.g. Chan 2005). The depression does lie in a region of poleward PV gradient, but this gradient seems fairly weak at the latitude of the depression. *This motivates the central question of this chapter: can the beta effect alone produce the azimuthally asymmetric vorticity needed for the northwestward advection of the 500 hPa PV structure?* Since composite averaging may obscure detailed relationships

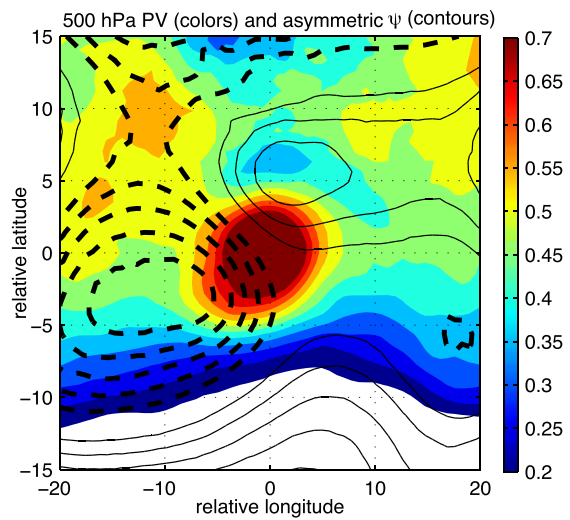


Fig. 8. Storm-centered composite mean PV (color shading, in PVU), and azimuthally asymmetric horizontal streamfunction (contours, negative dashed, interval $5 \times 10^5 \text{ m}^2 \text{ s}^{-1}$), both at 500 hPa.

between gradients and local maxima in the PV field, we next turn to a case study to shed light on this question.

First, though, we note that the anticyclonic gyre seen in the asymmetric streamfunction at 500 hPa is spatially coincident with a relative minimum of PV (Fig. 8). Horizontal advection alone cannot create such local minima in a conserved quantity, so one wonders if friction, vertical advection, or diabatic heating might be responsible. Hunt and Parker (2016) suggest that the low-level circulation of monsoon depressions may interact barotropically with Himalayan topography to produce northwestward motion of the depressions; they frame this mechanism in terms of image vortices, but one might relatedly argue that friction with the Himalayas produces this PV minimum. It is unclear whether this interaction could operate at 500 hPa (average plateau surface pressures are around 550 hPa); destruction of PV in the dry boundary layer over the Tibetan Plateau might also play a role. It is also unclear whether interaction with topography could explain the cyclonic gyre to the southwest of the PV maximum.

3.4. Case study of asymmetric gyre creation

At 500 hPa, the streamfunction minimum of the Sept. 2008 depression is centered slightly southwest of the PV maximum, and the PV field around the depression is relatively disorganized without a clear and strong meridional gradient at the latitude of the depression's center (Fig. 9a). The offset between the streamfunction minimum and PV maximum is more clearly seen in the component of the streamfunction that is azimuthally asymmetric about the PV maximum; that field shows an anomalous cyclone southwest of the PV maximum and an anomalous anticyclone to the northeast (Fig. 9b), highly similar to the structure seen in the composite mean (Fig. 8). The total wind at 500 hPa is indeed directed toward the northwest (blue vector in Fig. 9b), and has a magnitude and direction only slightly different from that of the storm propagation (red vector). The fact that the time mean wind (the green vector) is about an order of magnitude weaker and directed toward the southwest indicates that advection by the time mean wind has little relevance for translation of the 500 hPa PV maximum. All of these features are consistent with the composite-mean behavior discussed above, and with the idea that horizontal, nonlinear advection produces the northward motion of the depression.

Chan *et al.* (2002) employed similar reasoning in the context of tropical cyclones, and called this the “advection of symmetric PV by the asymmetric flow [AASPV, which includes, but is not limited to, the environmental ‘steering flow’ and the beta-induced circulation (the so-called ventilation flow)]”. Diabatic PV generation (and its subsequent vertical advection) shift the storm propagation vector only slightly to the southwest of the position it would have due to horizontal advection alone (Boos *et al.* 2015), indicating that the direct generation of PV by asymmetric heating plays little role in shifting the PV maximum directly.

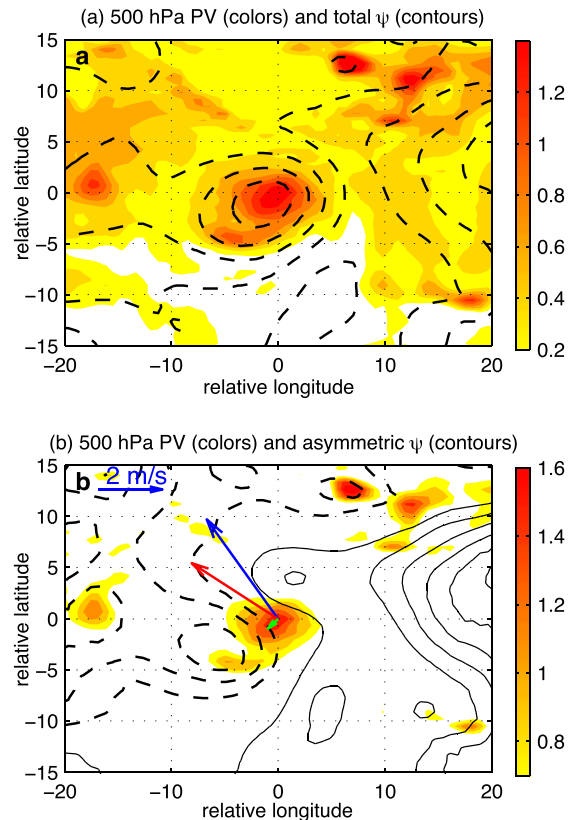


Fig. 9. For the 2008 depression at 1800 UTC on Sept. 16, in a storm-centered coordinate system: (a) total horizontal streamfunction at 500 hPa (contours, dashed negative, interval of $10^6 \text{ m}^2 \text{ s}^{-1}$) and 500 hPa PV (color shading); (b) as in (a) but the azimuthally asymmetric part of the streamfunction, with a contour interval of $5 \times 10^5 \text{ m}^2 \text{ s}^{-1}$. Blue arrow is the total horizontal wind vector, green arrow is the climatological mean horizontal wind vector, and red arrow is the storm propagation velocity; all wind vectors are PV-weighted averages taken over a $2 \times 2^\circ$ box centered on the PV maximum. Color shading in both panels shows the same PV field, but with a larger minimum contour in (b) to highlight the maxima.

However, we now suggest that this diabatic PV generation creates asymmetries in the flow field that allow for the adiabatic advection of the depression to the northwest. The relatively weak anticyclonic gyre northeast of the vortex center is not obviously associated with any negative PV anomaly, while the stronger cyclonic gyre to the southwest is roughly coincident with a “tail” of

high-PV air extending southwest of the central PV maximum. The meridional PV gradient west of the depression does not seem strong enough to allow for creation of the PV tail by horizontal adiabatic advection: again, advection cannot create extrema of conserved quantities.

This tail of high PV air lies in a region of strong vertical gradient of diabatic heating, as evidenced by depictions of the three-dimensional distribution of PV and the net diabatic heating rate in the EC-YOTC product (Fig. 10, and inset of Fig. 4a). The transect of estimated net diabatic heating rate in Fig. 10 shows that this tail of high PV might be formed in the mid-tropospheric vertical gradient of heating, not transported from a poleward reservoir of high PV as an adiabatic “beta drift” mechanism would imply. The vertical structure of diabatic heating is better seen in heating rates averaged over a region centered on the tail of high PV southwest of the vortex center (Fig. 11a). The large vertical gradient in diabatic heating at 500 hPa results primarily from a stratiform heating structure (Houze 1997) represented by grid-scale condensation and evaporation handled by the microphysics scheme in the EC-YOTC model. In contrast, the model’s parameterized convective heating peaks at 500 hPa, and has a vertical gradient that generates positive PV between the surface and 500 hPa, and negative PV between 500 hPa and the tropopause. The net PV tendency due to diabatic processes strongly resembles that due to the stratiform heating, with maximum PV generation at 500 hPa (Fig. 11b). Diabatic heat sources other than stratiform and convective heating (e.g. radiation) are comparatively small. There is net negative diabatic heating below 550 hPa, much of which results from the strength of the stratiform-like evaporative cooling.

To have the net diabatic heating be negative in the lower troposphere during tropical precipitation is not very typical of tropical convection, even in mesoscale systems where the heating profile is known to be top-heavy due

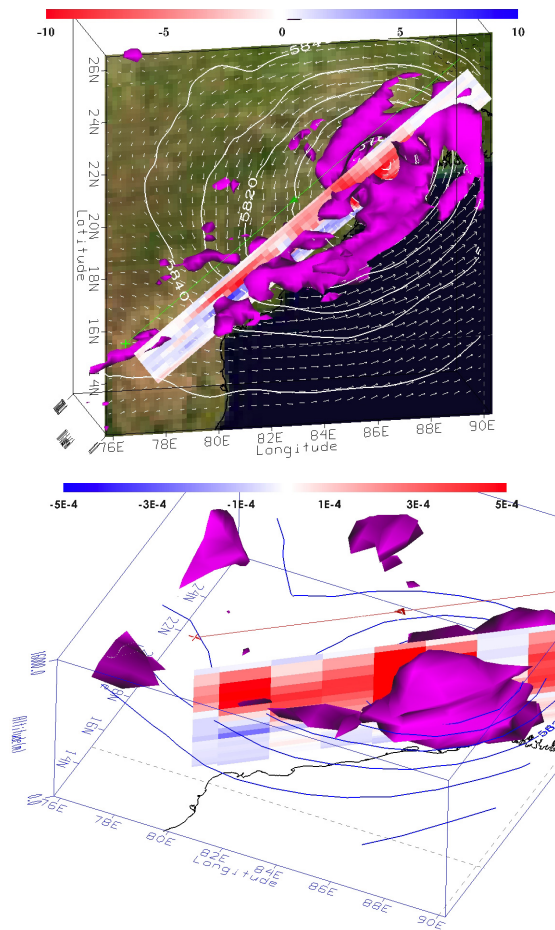


Fig. 10. Diabatic heating rate estimates from all physical processes in cross section (shading, red positive and blue negative, units K/s) through the rainy southwest quadrant of the Sept. 16, 2008 depression. The 1 PVU isosurface (magenta) is depicted from EC-YOTC (top) and MERRA (bottom), along with geopotential height contours at 500 hPa in both figures. In both depictions, the total heating is estimated to be negative in the lower troposphere (blue), indicative of a strong midlevel heating gradient (and associated PV source). In animations of both products (not shown), air with PV = 1 PVU appears to be formed in the midlevel vertical heating gradient and then advected downwind, not simply transported into the section from regions of high planetary vorticity to the north as an adiabatic “beta effect”.

to stratiform precipitation contributions (e.g. Houze 1989, 1997). An especially strong stratiform cooling at low levels perhaps results from dry lower tropospheric conditions over India

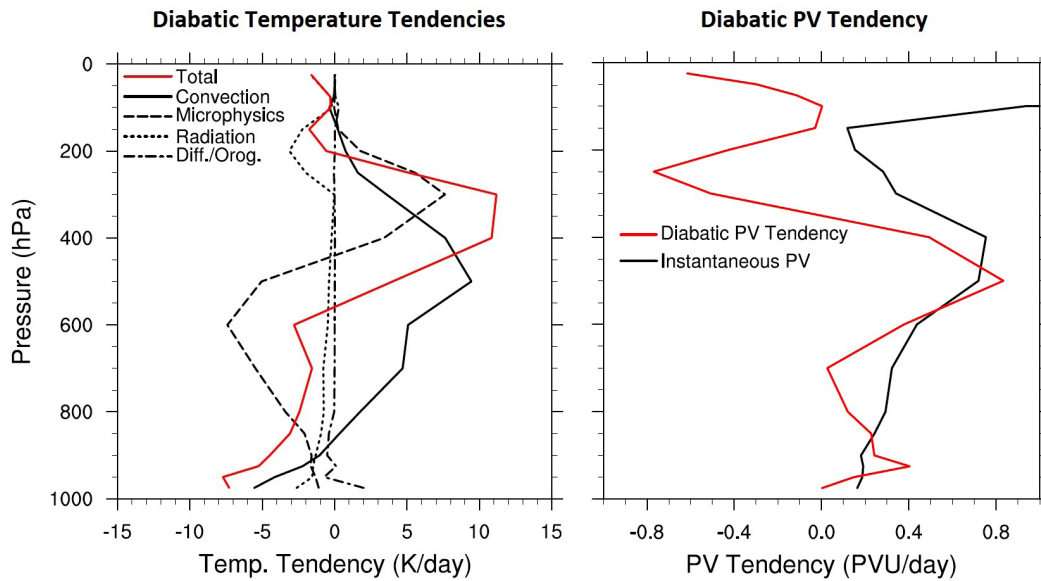


Fig. 11. Vertical profiles of EC-YOTC diabatic temperature tendencies (left) and diabatic PV tendency (right) in the region of high PV southwest of the vortex center during the monsoon depression of September 2008. The diabatic temperature tendency profiles are horizontally averaged in the region 15–19°N, 80–86°E at 1800 UTC on September 16, 2008. The diabatic PV tendency is the product of the absolute vorticity (not shown) and the vertical gradient of the diabatic temperature tendency; other components of the vorticity and potential temperature gradient vectors make a negligible contribution.

that allow for especially large evaporation of falling condensate. It is also possible that the ascent forced by the dynamics of the depression interacting with its sheared baroclinic environment, thought to be the reason for rain in the southwest quadrant, is more top-heavy than in typical deep-convectively driven stratiform precipitation. In a time-mean averaged over the center of the depression, rather than just its southwestern quadrant, the net diabatic heating is positive at nearly all levels even though the evaporative cooling is about 5 K day^{-1} throughout much of the lower troposphere (not shown).

Additional cases should be examined to determine how representative these analyses are of all monsoon depressions, and field data beyond gridded analyses would be helpful to add confidence to these results. Nevertheless, the distributions of PV, horizontal streamfunction, and diabatic heating in this case study suggest that diabatic heating rather than adiabatic advection

of planetary vorticity is needed to create the asymmetries in the flow field that adiabatically advect depressions to the northwest.

4. Conclusions

Indian monsoon depressions have traditionally been thought of as lower tropospheric relative vorticity maxima embedded in mean low-level westerlies, requiring some special mechanism to explain their apparent upstream, westward propagation. We have shown that these depressions can alternatively be viewed as PV maxima with peak amplitude in the middle troposphere. Since PV, unlike relative vorticity, is a conserved quantity that can be altered only by non-conservative diabatic heating and mechanical forcing, these PV maxima might be expected to be advected to the west by the mid- to upper-level easterly mean flow. However, the

climatological mean wind is weak compared to the total wind, indicating that nonlinear advection by flow associated with the depression is important.

Indeed, asymmetric gyres, especially a cyclonic gyre southwest of the PV maximum, are seen in the mid-tropospheric horizontal streamfunction, and the storm propagation vector is approximately equal to the total wind vector averaged over the 500 hPa PV maximum. This indicates that monsoon depressions propagate to the northwest primarily by advection of the vortex by an anomalous cyclone that, together with the peak precipitation, spreads off to the southwest of the vortex center. Diabatic PV generation by the precipitation does shift the PV maximum to the southwest slightly, but this has a comparatively minor effect on vortex motion, as shown by Boos *et al.* (2015). In the terminology of Wu and Wang's (2001) analysis of tropical cyclone motion, the "direct generation" of PV plays only a minor role in vortex motion, and instead diabatic advection "by heating-induced asymmetric flow" may be the key effect of precipitation-related heating. Three-dimensional structures of PV and diabatic heating in a case study were shown to suggest a scenario in which strong stratiform heating generates azimuthally asymmetric PV and associated balanced flow that produces the northwestward advection of the main center of the depression. Further examination of monsoon depression dynamics in observations and numerical models would help to determine whether this propagation mechanism operates more generally in monsoon depressions in India and other regions.

Acknowledgments

WRB and VSM acknowledge support from Office of Naval Research Young Investigator Program award N00014-11-1-0617 and National Science Foundation award AGS-1253222. BEM acknowledges financial support given by the

Earth System Science Organization, Ministry of Earth Sciences, Government of India (Grant no./Project no MM/SERP/Univ_Miami_USA/2013/INT-1/002) to conduct this research under Monsoon Mission.

References

- Berry, G. J., M. J. Reeder, and C. Jakob, 2012: Coherent synoptic disturbances in the Australian monsoon. *J. Climate*, **25**, 8409–8421.
- Boos, W. R., J. V. Hurley, and V. S. Murthy, 2015: Adiabatic westward drift of Indian monsoon depressions. *Quart. J. Roy. Meteor. Soc.*, **141**, 1035–1048. doi:10.1002/qj.2454.
- Chan, J. C. L., F. M. F. Ko, and Y. M. Lei, 2002: Relationship between potential vorticity tendency and tropical cyclone motion. *J. Atmos. Sci.*, **59**, 1317–1336.
- Chan, J. 2005: The physics of tropical cyclone motion. *Ann. Rev. Fluid Mechanics*, **37**, 99–128.
- Chen, T.-C., J.-H. Yoon, and S.-Y. Wang, 2005: Westward propagation of the Indian monsoon depression. *Tellus A*, **57**, 758–769.
- Dee, D. and coauthors, 2011: The ERA-Interim reanalysis: Configuration and performance of the data assimilation system. *Quart. J. Roy. Meteor. Soc.*, **137**, 553–597.
- Farrell, B., 1985: Transient growth of damped baroclinic waves. *J. Atmos. Sci.*, **42**, 2718–2727.
- Fiorino, M. and R. Elsberry, 1989: Some aspects of vortex structure related to tropical cyclone motion. *J. Atmos. Sci.*, **46**, 975–990.
- Godbole, R. V., 1977: The composite structure of the monsoon depression. *Tellus*, **29**, 25–40.
- Hodges, K., 1995: Feature tracking on the unit sphere. *Mon. Wea. Rev.*, **123**, 3458–3465.
- Houze, R. A., 1989: Observed structure of mesoscale convective systems and implications for large-scale heating. *Quart. J. Roy. Meteor. Soc.*, **115**, 425–461.
- Houze, R. A., Jr., 1997: Stratiform precipitation in regions of convection: A meteorological paradox? *Bull. Amer. Meteor. Soc.*, **78**, 2179–2196.
- Hunt, K. M. R. and D. J. Parker, 2016: The movement of Indian monsoon depressions by interaction with image vortices near the Himalayan wall. *Quart. J. Roy. Meteor. Soc.*, **142**, 2224–2229. doi:10.1002/qj.2812.
- Hurley, J. V. and W. R. Boos, 2015: A global climatology of monsoon low-pressure systems.

- Quart. J. Roy. Meteor. Soc.*, **141**, 1049–1064. doi:10.1002/qj.2447.
- India Meteorological Department, 2011: Tracks of cyclones and depressions over North Indian Ocean (from 1891 onwards). Technical Note, Regional Meteorological Centre, Chennai.
- Kalnay, E. and coauthors, 1996: The NCEP/NCAR 40-year reanalysis project. *Bull. Amer. Meteor. Soc.*, **77**, 437–470.
- Krishnamurti, T. N., R. J. Pasch, H.-L. Pan, S.-H. Chu, and K. Ingles, 1983: Details of low latitude medium range numerical weather prediction using a global spectral model I: Formation of a monsoon depression. *J. Meteorol. Soc. Japan*, **61**, 188–206.
- Krishnamurti, T. N., A. Martin, R. Krishnamurti, A. Simon, A. Thomas, and V. Kumar, 2013: Impacts of enhanced CCN on the organization of convection and recent reduced counts of monsoon depressions. *Clim. Dyn.* **41**: 117–134.
- Mooley, D. and J. Shukla, 1987: Characteristics of the westward-moving summer monsoon low pressure systems over the Indian region and their relationship with the monsoon rainfall. Tech Rep., University of Maryland, Department of Meteorology, Center for Ocean-Land-Atmosphere Interactions.
- Moorthi, S. and A. Arakawa, 1985: Baroclinic instability with cumulus heating. *J. Atmos. Sci.*, **42**, 2007–2031.
- National Hurricane Center, 2015: Glossary, accessed 5 April 2015, http://www.nhc.noaa.gov/about_gloss.shtml.
- Ramage, C. S., 1971: *Monsoon Meteorology*. Academic Press, New York.
- Rao K. and S. Rajamani, 1970: Diagnostic study of a monsoon depression by geostrophic baroclinic model. *Indian J. Meteor. Geophys.*, **21**, 187–194.
- Reinecker, M. M. and coauthors, 2011: MERRA: NASA’s Modern-Era Retrospective Analysis for Research and Applications. *J. Climate*, **24**, 3624–3648.
- Saha, S. and coauthors, 2010: The NCEP Climate Forecast System Reanalysis. *Bull. Amer. Meteor. Soc.*, **91**, 1015–1057.
- Sanders, F., 1984: Quasi-geostrophic diagnosis of the monsoon depression of 5–8 July 1979. *J. Atmos. Sci.*, **41**, 538–552.
- Sikka, D., 1977: Some aspects of the life history, structure and movement of monsoon depressions. *Pure Appl. Geophys.*, **115**, 1501–1529.
- Waliser, D. E. and coauthors, 2012: The “Year” of Tropical Convection (May 2008–April 2010). *Bull. Amer. Meteor. Soc.*, **93**, 1189–1218.
- Wang, B., R. L. Elsberry, W. Yuqing, and W. Liguang, 1998: Dynamics in tropical cyclone motion: A review. *Chinese J. Atmos. Sci.*, **22**, 416–434.
- Wu, L. and B. Wang, 2001: Effects of convective heating on movement and vertical coupling of tropical cyclones: A numerical study. *J. Atmos. Sci.*, **58**, 3639–3649.
- Yoon, J. H. and W.-R. Huang, 2012: Indian monsoon depression: Climatology and variability. In *Modern Climatology*, S.-Y. Wang, Ed., InTech, chap. 2, pp. 45–72.
- Yoon, J.-H. and T.-C. Chen, 2005: Water vapor budget of the Indian monsoon depression. *Tellus A*, **57**, 770–782.

